PHYSICAL REVIEW E VOLUME 62, NUMBER 4 OCTOBER 2000

Ferroelectric phases in a chiral bent-core smectic liquid crystal: Dielectric and optical second-harmonic generation measurements

E. Gorecka and D. Pociecha
Department of Chemistry, Warsaw University, Zwirki i Wigury 101, 02-089 Warsaw, Poland

F. Araoka, D. R. Link, M. Nakata, J. Thisayukta, Y. Takanishi, K. Ishikawa, J. Watanabe, and H. Takezoe
Department of Organic and Polymeric Materials, Tokyo Institute of Technology, O-okayama 2-12-1, Meguro-ku, Tokyo 152-8552, Japan

(Received 11 May 2000)

We report unambiguous evidence for ferroelectricity in a chiral bent-core liquid crystal. This evidence includes (i) a single current peak in the polarization reversal current, (ii) a strong dielectric response that is suppressed by applying a bias electric field, and (iii) strong optical second-harmonic generation in the absence of electric field even at normal incidence. We propose a phase structure that is anticlinic in tilt and ferroelectric in polar order, i.e., smectic-$C_A P_F^*$.

PACS number(s): 77.84.Nh, 61.30.Gd

Ferroelectricity in smectic liquid crystals has attracted great attention since it was predicted and shown to exist by Meyer *et al.* in 1975. In their experiments, ferroelectricity was realized by reducing the symmetry of the smectic-*C* (Sm-*C*) phase from C_{2h} to C_2 through the introduction of chiral molecules [1]. An alternative route to polar order was recently discovered in the fluid smectic phases of achiral bent-core molecules [2]. In these phases macroscopic orientational ordering of the bent-cores results in polar smectic layers. In the initial phases observed, the molecules within these layers were on average tilted synclinic with respect to the layer normal and antiferroelectric in polar order [3–9]. There have, however, been several ferroelectric analogs reported [10–12] which have all been realized in phases of asymmetric bent-core molecules, one of which has a chiral tail [12]. The conclusion of ferroelectricity in all these studies has been made based on the observation of a single peak in the polarization reversal current.

Here, we present distinct evidence for ferroelectric order observed in the symmetric chiral bent-core compound P8OPIMB6* (see Fig. 1), which exhibits ferroelectricity. The aim of this Rapid Communication is to clearly show the existence of the ferroelectric ordering of dipoles. A detailed report of the molecular ordering and electrooptic observations in this phase is in preparation [13]. In the present manuscript switching current, dielectric and optical second-harmonic generation (SHG) measurements clearly demonstrate polar order in the absence of an electric field *E*. Although this compound incorporates two chiral centers, their presence near the end of the alkyl chains is not expected to significantly effect the spontaneous electric polarization P_s.

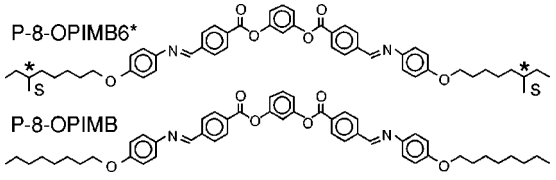

FIG. 1. Chemical structures for the chiral material P8OPIMB6* and achiral material P8OPIMB. The two chiral centers in P8OPIMB6* are indicated with asterisks.

The dipole moments that contribute to P_s come mainly from the ester groups at the central phenyl ring, as in the conventional phase of bent-core materials [8].

The cells for the dielectric, SHG and electrooptic measurements were prepared from indium-tin-oxide (ITO) coated glass plates separated by 2-, 4-, 10-, and 25-μm thick spacers, and were filled with P8OPIMB6* by capillary action in the isotropic phase.

The phase sequence of the compound as determined by differential scanning calorimetry (DSC) at a rate of 5 K/min is Sm-*Z** — 146.8 °C (16.86 J/g) — Sm-*Y** — 154.9 °C (2.36 J/g) — Sm-*X** — 166.8 °C (24.41 J/g) — Iso on heating and Iso — 166.6 °C — Sm-*X** — 146.2 °C — Sm-*Y** — 138.1 °C — Sm-*Z** on cooling. Preliminary x-ray studies indicate that the Sm-*X** and Sm-*Y** phases have nearly the same layer thickness ($d = 36.6$ Å) and that the Sm-*Z** phase is probably a crystalline phase ($d = 42.3$ Å). A simple estimate of the molecular length gives 43 Å, implying that the Sm-*Z** phase is untilted while the Sm-*X** and Sm-*Y** phases are tilted with a tilt angle $\theta \sim 30°$.

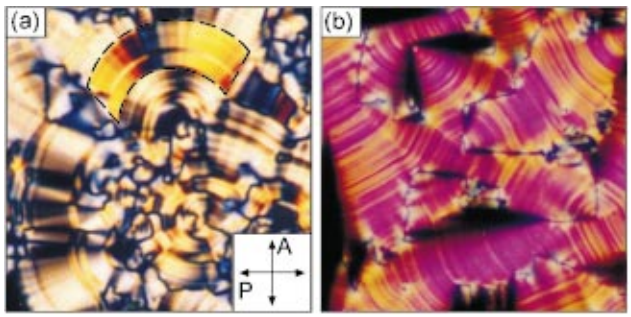

FIG. 2. (Color) Texture of the Sm-*X** phase (a) and Sm-*Z** phase (b) observed in a 4-μm-thick planar cell. Several types of domains can be observed in the Sm-*X** phase. The high birefringence (orange region surrounded by broken curve) domains in (a) are unstable and are rapidly converted into the low birefringence state upon application of an electric field. The low birefringence domains of the Sm-*X** phase, shown in (a), and all domains in the Sm-*Z** phase, shown in (b), have optic axes parallel to the layer normal.

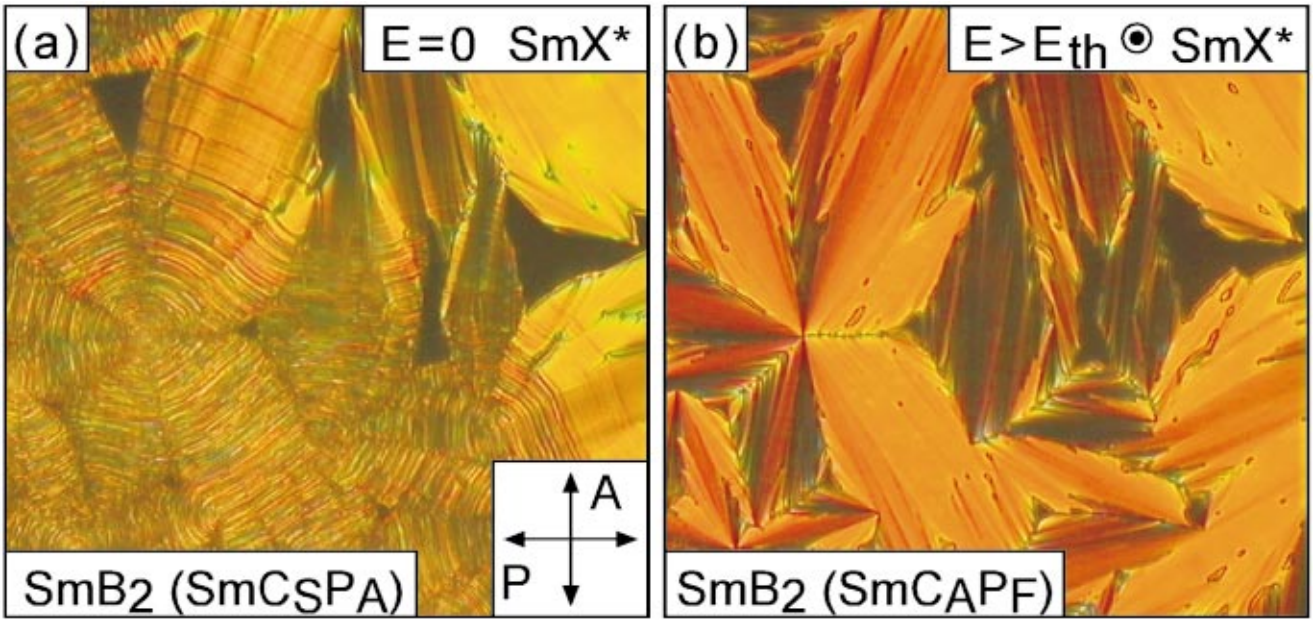

FIG. 3. (Color) Contact of chiral P8OPIMB6* in the Sm-X^* phase and its achiral analog P8OPIMB in the Sm-B_2 phase. In (a) a distinct boundary separates the two phases in the absence of an electric field, while in (b) this boundary disappears upon application of an electric field E.

In the Sm-X^* phase, on cooling from the isotropic phase in 4-μm-thick planar samples, a smooth pale-yellow fan texture of low birefringence is observed that coexists with a few bright color domains (high birefringence), as shown in Fig. 2(a). The majority of domains under a bipolar square or triangle wave electric field switch between states having the same birefringence, and extinction direction, which suggests an anticlinic tilt arrangement in neighboring layers in the field-on state. A small difference in birefringence was observed between the field-off and field-on states. No change in texture or switching behavior could be observed between the Sm-X^* and Sm-Y^* phases. The high-birefringence domains have different optical characteristics. However, they are not stable and are converted to the low-birefringence domains under application of an electric field for several minutes. Here we focus on the stable state, while the characteristics of the high-birefringence domains will be reported elsewhere [13].

A contact of the chiral P8OPIMB6* and its achiral analog P8OPIMB was prepared in a 10-μm-thick cell. In the absence of an electric field a distinct boundary separates the two materials [see Fig. 3(a)]. As shown in Fig. 3(b), this boundary disappears when an electric field greater than a threshold field E_{th} is applied to the cell, indicating that structure of the Sm-X^* phase of the chiral material is the same as its achiral analog in the presence of $E>E_{th}$, i.e., when the director in adjacent layers is tilted anticlinic [3]. Moreover, the electric field required to switch the Sm-X^* phase ($0.3\,\mathrm{V}/\mu\mathrm{m}$ in a 25-μm-thick cell and $2.0\,\mathrm{V}/\mu\mathrm{m}$ in a 10-μm-thick cell) is much weaker than the electric field necessary to switch the Sm-B_2 (Sm-$C_S P_A$) phase of P8OPIMB ($\sim 5\,\mathrm{V}/\mu\mathrm{m}$). We observe an increase in birefringence at the Sm-Y^* to Sm-Z^* phase transition. The Sm-Z^* phase does not show an electrooptic response.

In addition to the texture observations three methods were used to probe the ferroelectric order in the Sm-X^* phase. Those being (i) switching current, (ii) dielectric and (iii) SHG measurements. The first of these provides us with direct evidence for ferroelectricity. For the chiral P8OPIMB6* a single peak in the polarization reversal current is observed under application of a triangle wave voltage (at frequencies from several Hz to several hundred Hz), as shown in Fig. 4, indicating ferroelectricity. Under the same conditions a double peak is observed in the Sm-B_2 phase of its antiferroelectric achiral analogue [4,6,8,9]. The spontaneous polarization P_s measured in P8OPIMB6* is $\sim 500\,\mathrm{nC/cm^2}$, and does not change meaningfully with temperature.

The second evidence for ferroelectricity was obtained by dielectric studies. The complex dielectric permittivity $\varepsilon^*(\omega)=\varepsilon'-i\varepsilon''$ was measured over 20 Hz–300 kHz frequency range. The relaxation frequency f_r and dielectric strength $\Delta\varepsilon$ of the mode were evaluated by fitting the data to the Cole-Cole formula

$$\varepsilon^*-\varepsilon_\infty=\frac{\Delta\varepsilon}{1+(if/f_r)^{(1-\alpha)}}-i\frac{\sigma}{2\pi\varepsilon_0 f}, \tag{1}$$

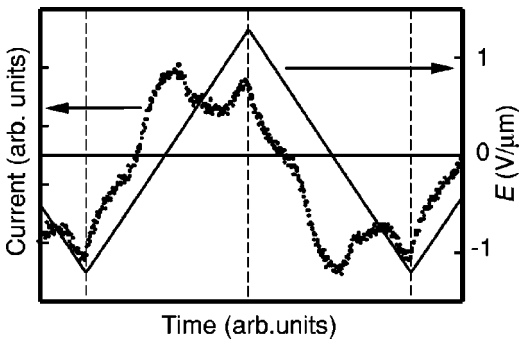

FIG. 4. Polarization reversal current in the Sm-X^* phase. The single current peak on application of a triangle wave indicates ferroelectric switching. The applied electric field is $2.5\,\mathrm{V}/\mu\mathrm{m}$ at a frequency of 5 Hz, 10 °C below the isotropic transition temperature.

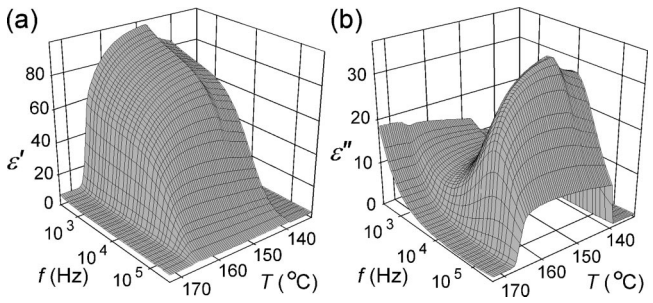

FIG. 5. Frequency f and temperature T dependence of the real ε' (a) and imaginary ε'' (b) parts of the complex dielectric permittivity measured on cooling in a 2-μm-thick cell.

where α and ε_∞ are respectively the distribution parameter of the mode and a permittivity at an infinite frequency.

In the Sm-X* and Sm-Y* phases a strong relaxation mode ($\Delta\varepsilon \sim 80$ even in a 2-μm-thick cell) was observed at a frequency f_r on the order of several tens of kHz, as is shown in Fig. 5. Fitting gave $\alpha \sim 0.1$ throughout the entire temperature range indicating a single relaxation mode. In the 2-μm-thick cell at the Sm-X* to Sm-Y* phase transition temperature on cooling, the relaxation frequency increases slightly while the dielectric strength decreases. With increasing cell thickness the strength of the mode increases and the relaxation frequency shifts to lower values, but the qualitative trends remain the same. The frequency of the mode fit to the Arhenius law $f = f_0 e^{-E_a/k_B T}$, where k_B is Boltzman's constant, in the temperature ranges 139–143 °C (Sm-Y*) and 147–158 °C (Sm-X*) gave the activation energies E_a of

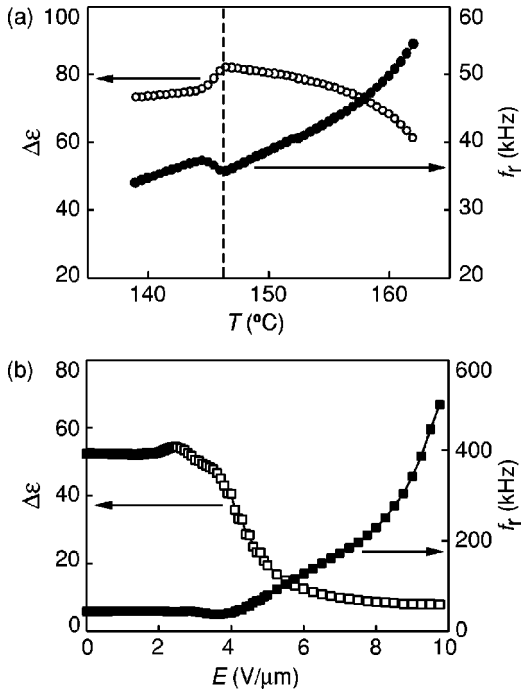

FIG. 6. Relaxation frequency f_r (closed symbols) and dielectric strength $\Delta\varepsilon$ (open symbols) in a 2-μm-thick cell. The temperature dependence of f_r and $\Delta\varepsilon$ on cooling is shown in (a). The dashed vertical line indicates the Sm-X* to Sm-Y* phase transition temperature. (b) The bias field dependence of the relaxation frequency and dielectric strength in the Sm-X* phase 5 °C below the transition from the isotropic phase.

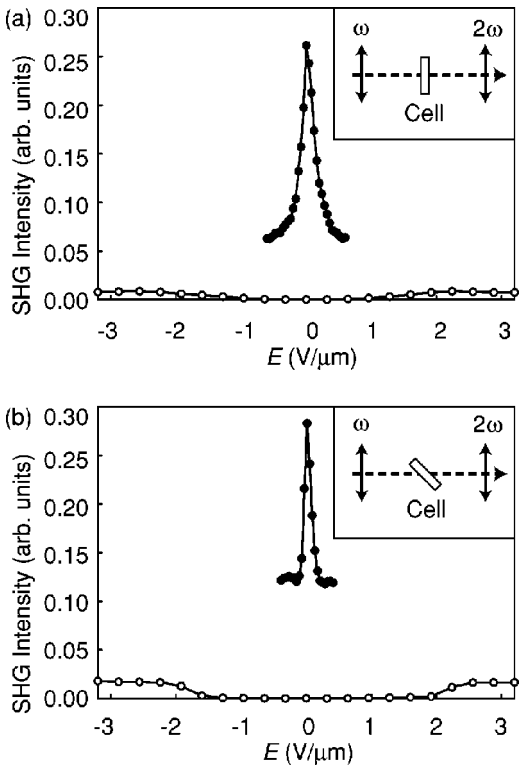

FIG. 7. SHG intensity as a function of an applied electric field. The closed and open circles represent the signal for the chiral (P8OPIMB6*) and achiral (P8OPIMB) compounds, respectively. The SHG signal was measured 5 °C below the transition from the isotropic phase. The insets show the polarization of light and optical geometry of the measurements.

25 J/mol and 34 J/mol, respectively. These energies are about half of that reported for rotation around long molecular axis of antiferroelectric bent-core molecules [14] and comparable to the value obtained from the temperature dependence of relaxation frequency for the Goldstone mode in the regular chiral Sm-C* phase. The low activation energies, high dielectric strength and low relaxation frequency of the mode suggest collective fluctuations. By applying a bias electric field above a critical value ($E_c = 3.7\,\mathrm{V}/\mu\mathrm{m}$), the mode is damped and the relaxation frequency increases, as shown in Fig. 6. This is typical in ferroelectric phases and is the result of the bias field suppressing fluctuations in the polarization. This behavior is the opposite of that observed in the conventional antiferroelectric Sm-B_2 phase, where $\Delta\varepsilon$ increases with increasing bias field as a response to field-induced distortions in the perfect antiferroelectric order that produces a polarization [9]. Thus, these dielectric observations strongly indicate that the Sm-X* and Sm-Y* phases have ferroelectric polar order.

The third probe used to investigate the polar order of P8OPIMB6*, SHG, also indicates ferroelectric polar order. The SHG signal from the cells was measured from the incidence of a fundamental light of a neodymium-doped yttrium aluminum garnet (Nd-YAG) laser of wavelength $\lambda = 1064$ nm. The repetition rate was 10 Hz and the intensity was 0.4 mJ/pulse. The beam was not focused, so that multidomains exist inside a 2-mm-diameter beam spot. Measurements were made with normal incidence and 45° oblique

incidence as a function of electric field E applied normal to the cell for both P8OPIMB6* and P8OPIMB. The transmitted intensity of p-polarized second-harmonic light was observed from p-polarized fundamental light incident at 0° [see Fig. 7(a)] and at 45° [see Fig. 7(b)] to the cell normal. In comparing the electric field dependence for the SHG signal observed from the Sm-B_2 and Sm-X^* phases, we note the following three characteristics: (i) The SHG signal gives a maximum at $E=0$ in the Sm-X^* phase, while in the Sm-B_2 phase it is almost zero at $E=0$; (ii) there is no threshold in the electric field dependence in the Sm-X^* phase, while the Sm-B_2 phase has one; and (iii) the maximum signal is an order of magnitude larger in the Sm-X^* phase in comparison to that in the Sm-B_2 phase. It is important to note that a strong SHG signal was observed even with normal incident light in the Sm-X^* phase while no such signal was observed in the Sm-B_2 phase. These results unambiguously indicate polar order in the Sm-X^* phase of P8OPIMB6* and that the spontaneous polarization has a component in the plane of the cell in the absence of an electric field. We propose that this zero-field state is stabilized by a preference for the polarization at the surfaces to align parallel to the cell normal, requiring it to rotate through π from top to bottom of the cell and to lie in the plane of the cell at the center point [13].

The texture observations including contact studies and layer thickness measurements suggest that the Sm-X^* and Sm-Y^* phases are tilted. Furthermore, the single current peak observed during P_s reversal, the high value of dielectric permittivity and the dielectric mode suppression by a bias field as well as the strong SHG activity in the absence of a field are consistent with the proposed ferroelectric structure, i.e., anticlinic tilt of molecules in neighboring layers and ferroelectric polar ordering.

Although the assignment of the exact mode observed in the dielectric measurements is somewhat ambiguous, we speculate that it is the collective motion of molecules on the tilt cone, i.e., the Goldstone mode. Ideally, the Goldstone mode should have a relaxation frequency $f_r \sim 0$ as it is due to fluctuations in an energetically degenerate state. However, this mode can shift to higher frequency, if a helical or surface induced twist structure is present or in the case of low rotational viscosity [15,16]. In typical ferroelectric tilted smectic phases (Sm-C^*) the Goldstone mode is observed at relaxation frequencies ranging from 0.1 to 10 kHz. For the ferroelectric phases of P8OPIMB6* this mode could be shifted to relatively high frequencies (35 to 55 kHz) due to low viscosity. Low viscosity is suggested by the very fast switching time (less than 10 μs under a field of 10 V/μm). However, there is no evidence that a helix is present in either the Sm-X^* or Sm-Y^* phase. A second possible assignment of this mode is to a collective rotation around the molecular long-axis without changing the tilt direction. In this case it is expected that the mode is shifted to higher frequency, since it is not connected to the fluctuations around energetically degenerated ground state. Irrespective of the two possible assignments, the relaxation mode is clearly related to fluctuations in P_s, indicating a ferroelectric structure.

In summary, based on switching current, dielectric and SHG measurements, we conclude that the Sm-X^* phase is ferroelectric and propose that its ground state structure is anticlinic ferroelectric, Sm-$C_A P_F^*$.

We would like to thank Professor D. M. Walba for providing us with a preprint of his work. This work is partly supported by the NEDO International Collaboration Fund, a Grant-in-Aid for Scientific Research from the Ministry of Education, Science and Culture and Grant No. 3 T09A 04615 from the Polish State Committee for Scientific Research.

[1] R. B. Meyer, L. Liebert, L. Strzelecki, and P. Keller, J. Phys. (France) **36**, L-69 (1975).

[2] T. Niori, T. Sekine, J. Watanabe, and H. Takezoe, J. Mater. Chem. **6**, 1231 (1996).

[3] D. R. Link, G. Natale, R. Shao, J. E. Maclennan, N. A. Clark, E. Körblova, and D. M. Walba, Science **278**, 1924 (1997).

[4] S. Diele, S. Grande, H. Kruth, Ch. Lischka, G. Pelzl, W. Weissflog, and I. Wirth, Ferroelectrics **212**, 169 (1998).

[5] R. Macdonald, F. Kentischer, P. Warnick, and G. Heppke, Phys. Rev. Lett. **81**, 4408 (1998).

[6] G. Pelzl, S. Diele, S. Grande, A. Jakli, Ch. Lischka, H. Kresse, H. Schmalfuss, I. Wirth, and W. Weissflog, Liq. Cryst. **26**, 401 (1999).

[7] W. Weissflog, Ch. Lischka, S. Diele, G. Pelzl, and I. Wirth, Mol. Cryst. Liq. Cryst. **328**, 101 (1999).

[8] G. Pelzl, S. Diele, and W. Weissflog, Adv. Mater. **11**, 707 (1999).

[9] M. Zennyoji, Y. Takanishi, K. Ishikawa, J. Thisayukta, J. Watanabe, and H. Takezoe, Jpn. J. Appl. Phys. **39**, 3536 (2000).

[10] D. Shen, S. Diele, I. Wirt, and C. Tschierske, Chem. Commun. (Cambridge) **23**, 2573 (1998). This material was later reported to be antiferroelectric in D. Shen, A. Pegenau, S. Diele, I. Wirth, and C. Tschierske, J. Am. Chem. Soc. **122**, 1593 (2000).

[11] J. P. Bedal, H. T. Nguyen, J. C. Rouillon, J. P. Marcerou, G. Sigaud, and P. Barois, Mol. Cryst. Liq. Cryst. **332**, 163 (1999).

[12] D. M. Walba, E. Körblova, R. Shao, J. E. Maclennan, D. R. Link, M. A. Glaser, and N. A. Clark, Science **288**, 2181 (2000).

[13] M. Nakata, D. R. Link, F. Araoka, J. Thisayukta, Y. Takanishi, K. Ishikawa, J. Watanabe, and H. Takezoe (unpublished).

[14] H. Scmalfuss, D. Shen, and C. Tscheirske, Liq. Cryst. **26**, 1767 (1999).

[15] D. I. Uzunov, *Introduction to the Theory of Critical Phenomena* (World Scientific, Singapore, 1993).

[16] M. Zennyoji, J. Yokoyama, Y. Takanishi, K. Ishikawa, H. Takezoe, and K. Itoh, Jpn. J. Appl. Phys. **37**, 6071 (1998); B. Žekš and R. Blinc, in *Ferroelectric Liquid Crystals*, edited by G. W. Taylor (Gordon and Breach, Philadelphia, 1991).